V European Conference on Computational Fluid Dynamics
ECCOMAS CFD 2010
J. C. F. Pereira and A. Sequeira (Eds)
Lisbon, Portugal,14-17 June 2010

REALISTIC CONSTITUTIVE LAWS FOR POLYMER FLOWS

Didier Graebling

IPREM/EPCP, UMR CNRS 5154 Université de Pau et des Pays de l'Adour 2 avenue Angot
64053 Pau Cedex 9 (France) & INRIA Bordeaux-Sud-Ouest - Équipe Projet Concha (France)
e-mail: didier.graebling@univ-pau.fr

Key words: Polymer flows, rheological behaviour, Oldroy-B model, PTT model, Giesekus model, Weissenberg number

Abstract. *The flows of polymer liquid are not described by the Navier-Stokes equations because these liquid are characterized by a non-Newtonian behaviour. The rheological behaviour of a polymer liquid can be described by two forms of differential constitutive equations: quasi-linear differential models (UCM, Oldryod-B...) or the non-linear differential models (Phan-Thien and Tanner, Giesekus...). The quasi-linear models are not able to simulate the flow of polymer liquids. For example, the Oldroyd B liquid predicts a Newtonian viscosity in the case of a steady shear flow. Only, the non-linear constitutive equations like the Giesekus model gives a realistic description of the polymer flows. We show various numerical results for affine Phan-Thien and Tanner model and Giesekus model for three 2D planar flows: a simple channel, a 4:1 abrupt contraction and a 4:1:4 abrupt contraction/expansion. For a simple channel, the velocity profiles obtained by simulation are in good accordance with the analytical solutions for the fully developed flow. For contraction flows, the simulation results conform to reality.*

1 INTRODUCTION

The rheological complexity exhibited by polymeric liquid could be explained by a large number of constitutive equations. Theses laws are typically divided into three groups: The generalized Newtonian fluid, the quasi-linear models and the non-linear models. The most important property of polymeric fluids is the non-Newtonian viscosity. The generalized Newtonian constitutive equations can describe the idea of a shear rate dependent viscosity and they cannot describe the viscoelastic effects such as memory effect or normal stress (Weissenberg effect). The quasi-linear and the non-linear models can describe all the entire viscoelastic properties of these liquids. These models are constructed from linear viscoelastic models by employing the frame invariance concept. The main drawback of quasi-linear models is that they are generally valid for one type of flow (shear or elongational). Only, the non-linear models give a realistic description of polymer melt.

The polymer flow is essentially characterized by the Weissenberg number, $\mathfrak{We}$, defined by $\mathfrak{We} = \lambda\dot{\gamma}$, where λ is the relaxation time and $\dot{\gamma}$ is the shear-rate. $\mathfrak{We}$ gives information related to the molecular anisotropy and orientation in the flow[1].

Despite numerous efforts, computational non-Newtonian fluid mechanics is still a very challenging research area. The high-Weissenberg number problem (HWNP) is one of the main difficulties encountered in the numerical simulation of the polymer flows. The source of the problem is the breakdown in convergence of the algorithms at critical values of the Weissenberg number. The frustratingly low value of the Weissenberg number limits the CFD use for the polymer processing industry[11, 20].

Recently, it has been shown that the breakdown in convergence is related with the lack of positivity of the so-called conformation tensor at the discrete level[19, 14]. The conformation tensor can be interpreted as a tensorial measure of the molecular orientation and stretching of the chain. This tensor denotes the average of the dyadic product of the end-to-end vector of a polymer chain. In the last few years, numerical schemes preserving the positive definiteness of the discrete conformation tensor have been proposed in the literature[6, 9, 5, 12, 3]. Those methods lead to stongly nonlinear reformulations of the considered problems and therefore, their computation is very costly.

In this work, we consider a non-conforming finite element method to approach the velocity and the pressure and dG finite elements do approach the stress tensor for three kinds of viscoelastic liquids: The Oldroyd-B, the simplified version of the Phan-Thien and Tanner model[18, 17] and the Giesekus model[7, 8].

We have implemented this method in the homemade C++ library Concha ($http : //uppa - inria.univ - pau.fr/concha/$). The main objective of this project is the development of innovative algorithms and efficient software tools for the simulation of complex flow problems. A part of this work is devoted to the numerical simulation of polymer flows.

[1]Reynolds numbers between 10^{-4} and 10^{-1} are typical values for polymer flow.

2 GOVERNING EQUATIONS

In the case of incompressible isothermal flows, the motion of a liquid is described by :

- the mass conservation law,

$$\nabla \cdot \boldsymbol{u} = 0, \tag{1}$$

  where $\boldsymbol{u}$ is the velocity of the liquid.

- the momentum conservation law,

$$\rho\left(\frac{\partial}{\partial t}\,\boldsymbol{u} + \boldsymbol{u}\cdot\nabla\boldsymbol{u}\right) - \nabla\cdot\boldsymbol{\tau} + \nabla p = \boldsymbol{0}, \tag{2}$$

  where $\boldsymbol{\tau}$, p and ρ are respectively the extra-stress tensor, the pressure and the density of the fluid.

- and a constitutive equation.

The rheological behaviour of a polymer liquid can be adequately described by two types of differential constitutive equations:

- the quasi-linear differential models:

$$\boldsymbol{\tau} + \lambda\,\overset{\square}{\boldsymbol{\tau}}_a = 2\eta\,\boldsymbol{D} \tag{3}$$

  with $\overset{\square}{\boldsymbol{\tau}}_a$ the Gordon-Schowalter convected derivative of the extra-stress tensor.

- the nonlinear differential models:

$$f(\boldsymbol{\tau}) + \lambda\,\overset{\triangledown}{\boldsymbol{\tau}} = 2\eta\,\boldsymbol{D} \tag{4}$$

  with $f(\boldsymbol{\tau})$ a nonlinear function of the extra-stress tensor.

$\boldsymbol{D}$ is the Oldroyd strain-rate tensor defined by $\boldsymbol{D} = \frac{1}{2}\left\{\boldsymbol{\nabla u} + (\boldsymbol{\nabla u})^t\right\}$. η and λ are respectively the zero-shear viscosity and the relaxation time of the polymer liquid.

The Gordon-Schowalter convected derivative of the tensor $\boldsymbol{A}$ associated with the frame invariance concept, is defined by the following relationship:

$$\overset{\square}{\boldsymbol{A}}_a = \frac{\partial}{\partial t}\,\boldsymbol{A} + \boldsymbol{u}\cdot\boldsymbol{\nabla A} + \boldsymbol{A}\cdot\boldsymbol{\Omega} - \boldsymbol{\Omega}\cdot\boldsymbol{A} - a\left\{\boldsymbol{A}\cdot\boldsymbol{D} + \boldsymbol{D}\cdot\boldsymbol{A}\right\} \tag{5}$$

where a is a parameter $\in [-1, 1]$. $\boldsymbol{\Omega}$ is the vorticiy tensor defined by $\boldsymbol{\Omega} = \frac{1}{2}\left\{(\boldsymbol{\nabla u})^t - \boldsymbol{\nabla u}\right\}$

According to the chosen values for a, we obtain:

$$\begin{cases} \text{the upper-convected derivative for } a = 1: \\ \quad \overset{\triangledown}{\boldsymbol{\tau}} = \frac{\partial}{\partial t}\boldsymbol{\tau} + \boldsymbol{u}\cdot\boldsymbol{\nabla}\boldsymbol{\tau} - \left\{\boldsymbol{\tau}\cdot\boldsymbol{\nabla}\boldsymbol{u} + (\boldsymbol{\nabla}\boldsymbol{u})^t\cdot\boldsymbol{\tau}\right\} \\ \text{the Jaumann or co-rotational derivative for } a = 0: \\ \quad \overset{\circ}{\boldsymbol{\tau}} = \frac{\partial}{\partial t}\boldsymbol{\tau} + \boldsymbol{u}\cdot\boldsymbol{\nabla}\boldsymbol{\tau} + \boldsymbol{\tau}\cdot\boldsymbol{\Omega} + \boldsymbol{\Omega}\cdot\boldsymbol{\tau} \\ \text{lower-convected derivative for } a = -1: \\ \quad \overset{\triangle}{\boldsymbol{\tau}} = \frac{\partial}{\partial t}\boldsymbol{\tau} + \boldsymbol{u}\cdot\boldsymbol{\nabla}\boldsymbol{\tau} + \boldsymbol{\tau}\cdot(\boldsymbol{\nabla}\boldsymbol{u})^t + \boldsymbol{\nabla}\boldsymbol{u}\cdot\boldsymbol{\tau} \end{cases} \tag{6}$$

If we replace the time derivative by an objective time derivative, a linear model such as the Maxwell model could be transformed into a quasi-linear model, such as UCM model.

We consider three kinds of fluids, one quasi-linear: The Oldroyd-B model and two non-linear: the simplified version of the Phan-Thien and Tanner model[18][17] and the Giesekus model[7][8].

The constitutive equation of the Oldroyd-B model is:

$$\boldsymbol{\tau} + \lambda_t \overset{\triangledown}{\boldsymbol{\tau}} = 2\eta\left\{\boldsymbol{D} + \lambda_r \overset{\triangledown}{\boldsymbol{D}}\right\} \tag{7}$$

where η is the viscosity of the liquid. λ_t and λ_r are respectively the relaxation time and the retardation time of the fluid. It is assumed that $\lambda_t \geqslant \lambda_r \geqslant 0$.

For steady shear flow, the polymer melt behaviour cannot be adequately described by this model: Newtonian behaviour with a constant first normal-stress difference[2] $\Psi_1(\dot{\gamma}) = 2\eta\,(\lambda_t - \lambda_r)$ and without second normal-stress difference. In the case of an elongational flow, this model described reasonably the polymer melt behaviour: a Troutonian behaviour for $\dot{\varepsilon} < 1/2\lambda_t$ and a strain hardening for $\dot{\varepsilon} > 1/2\lambda_t$. The upper-convected Maxwell model is a limiting case of this model when $\lambda_r = 0$. The Oldroyd-B model is not able to simulate the flow of polymer liquids and more complex models have to be employed.

According to the choice of the function $f(\boldsymbol{\tau})$ (4), we obtain the two non-linear models used:

- the simplified or affine Phan-Thien and Tanner model (PTT):

$$f(\boldsymbol{\tau}) = \left(1 + \frac{\epsilon\lambda}{\eta}\,\mathrm{tr}\,\{\boldsymbol{\tau}\}\right)\boldsymbol{\tau} \quad \Rightarrow \quad \boldsymbol{\tau} + \frac{\epsilon\lambda}{\eta}\,\mathrm{tr}\,\{\boldsymbol{\tau}\}\,\boldsymbol{\tau} + \lambda\overset{\triangledown}{\boldsymbol{\tau}} = 2\eta\,\boldsymbol{D} \tag{8}$$

  where λ and ϵ are respectively the relaxation time and a non-dimensional adjustable parameter called the extensional parameter.

[2]Weissenberg effect.

- the Giesekus model:

$$f(\boldsymbol{\tau}) = \boldsymbol{\tau} + \frac{\alpha}{G}\,\boldsymbol{\tau}\cdot\boldsymbol{\tau} \quad \Rightarrow \quad \boldsymbol{\tau} + \frac{\alpha}{G}\,\boldsymbol{\tau}\cdot\boldsymbol{\tau} + \lambda\,\overset{\triangledown}{\boldsymbol{\tau}} = 2\eta\,\boldsymbol{D} \tag{9}$$

  where λ and α are respectively the relaxation time and a constant $\in [0, 1]$.

For a steady shear flow, the simplified form of the PTT model predicts a pseudoplastic behaviour, a first normal-stress difference function of the shear-rate and a zero second normal-stress difference. In the case of an elongational flow, this model describes suitably the polymer melt behaviour. The parameter ϵ imposes an upper limit to the elongational viscosity which becomes inversely proportional to this parameter. If the extensional parameter is set to zero, the Johnson-Segalman constitutive equation is recovered[10][13].

The Giesekus constitutive equation describes accurately a large panel of material functions. In the case $\alpha = 0.5$, this relatively simple constitutive equation predicts a pseudoplastic behaviour with the first and second normal-stress differences function of the shear-rate. This model predicts, in the case of an elongational flow, a Troutonian behaviour and a strain hardening with a finite asymptotic value. Setting $\alpha = 0$ reduces the model to the upper convected Maxwell model.

3 NUMERICAL METHOD

We consider a velocity-pressure-stress tensor formulation of the previous models. Our choice of the discrete spaces is based on a previous analysis on Newtonian flows[2]. Indeed, we have studied a dG approximation of the underlying three-fields Stokes problem related with a non-conforming method. However, the computation is very costly and therefore, the method is not well-adapted for three-fields formulations. Based on to the optimal theoretical and numerical results obtained, we have chosen to use here a combination of these two finite element methods.

The velocity and the pressure are approximated by non-conforming finite elements of Crouzeix-Raviart[4] while the stress tensor is approximated by P_0 discontinuous finite elements. The nonlinear problem is solved by means of Newton's method.

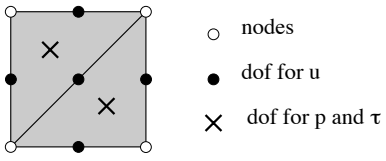

Figure 1: Degrees of freedom

4 RESULTS AND DISCUSSION

4.1 Geometries

In our simulations, three different planar flow rate configurations were studied: a simple channel, a 4:1 abrupt contraction and a 4:1:4 abrupt contraction/expansion. The dimensional characteristics and the definition of boundaries of these geometries are given in Figure 2 with 1 mm as value of a.

The boundary conditions are defined as follow: Inflow on Γ_1, flat velocity profil typically 0.1 m/s, homogeneous Dirichlet boundary conditions on Γ_2, outflow, Neumann boundary condition on Γ_3 and Symmetry plane on Γ_4.

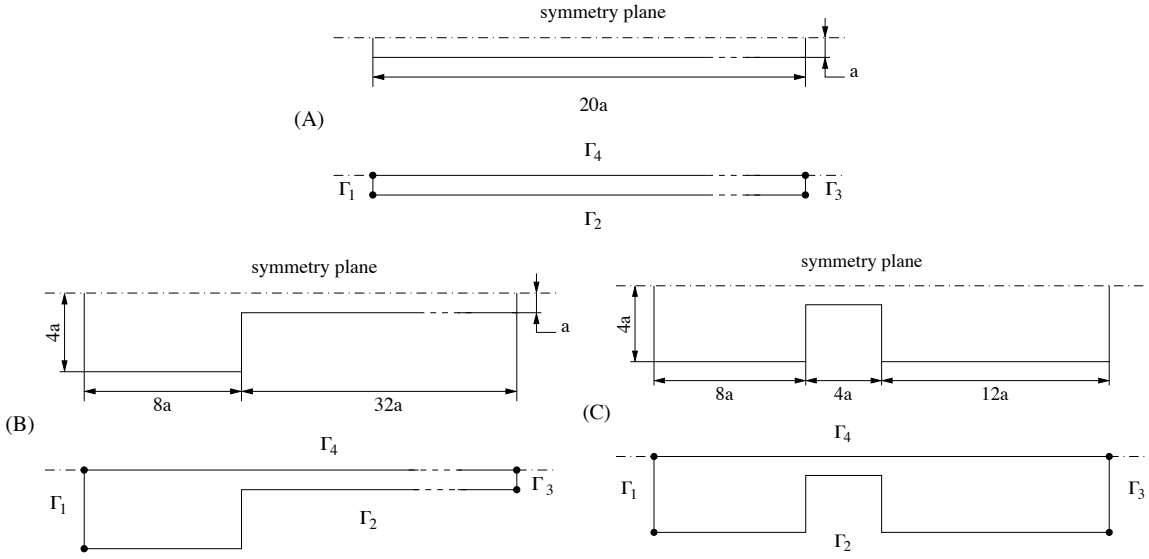

Figure 2: Geometries : (A) channel, (B) 4:1 contraction & (C) 4:1:4 contraction/expansion

4.2 Implementation of the model

Let's recall that our main goal is to obtain realistic results for high Weissenberg number. The Newton method does not converge if we consider directly a large Weissenberg number. To avoid this problem, we consider two approaches: Evolution or time-dependent simulations. For the evolution case, the code start the calculation using an existing results file computed with a smaller value of λ as an initial solution. At each step, the λ gap is fitted to obtain the convergence of the Newton method. In the case of time-dependent simulation, we impose λ as a constant and we controle the inlet velocity as a function of time:

$$\boldsymbol{u} \cdot \boldsymbol{n} = \bar{u} \left(1 - \mathrm{e}^{-\beta t}\right) \tag{10}$$

where, $\bar{u}$ is the mean velocity and β is a growth rate parameter.

4.3 Channel

To validate our approach, we compare the computed velocity profile and the analytical solutions for the fully developed channel flow. For this flow, the Weissenberg number is defined by:

$$\mathfrak{We} = \lambda\dot{\gamma} = \lambda\,\frac{3\bar{u}}{a}$$

where $\bar{u}$ is the inflow velocity or the average velocity on the channel. The shear-rate is calculated for the equivalent Newtonian liquid.

For the affine Phan-Thien and Tanner model, the velocity profile is given by the following relationship[16]:

$$u_x(y) = -\frac{a^2}{2\eta}\left(1-\frac{y^2}{a^2}\right)\left(1+\frac{\epsilon\lambda^2}{\eta^2}\,a^2\,\left(1+\frac{y^2}{a^2}\right)\,\left(\frac{\partial p}{\partial x}\right)^2\right)\frac{\partial p}{\partial x} \tag{11}$$

and the average velocity by:

$$\bar{u} = -\frac{a^2}{3\eta}\left(1+\frac{6}{5}\,\frac{\epsilon\lambda^2}{\eta^2}\,a^2\,\left(\frac{\partial p}{\partial x}\right)^2\right)\frac{\partial p}{\partial x} \tag{12}$$

The Weissenberg number is given by:

$$\mathfrak{We} = -\frac{\lambda a}{\eta}\left(1+\frac{6}{5}\,\frac{\epsilon\lambda^2}{\eta^2}\,a^2\,\left(\frac{\partial p}{\partial x}\right)^2\right)\frac{\partial p}{\partial x} \tag{13}$$

The pressure gradient is the real solution of the cubic equations (12) or (13).

In the case of the Giesekus liquid, a analytical solution is given by[15]:

$$u_x(y) = \frac{1}{4\beta\lambda^2}\,\ln\frac{1-4a^2\beta^2\lambda^2}{1-4y^2\beta^2\lambda^2}, \quad \beta = \frac{1}{2\eta}\,\frac{\partial p}{\partial x} \tag{14}$$

and the average velocity by:

$$\bar{u} = \frac{1}{2\beta\lambda^2}\left(1-\frac{\operatorname{atanh}(2a\beta\lambda)}{2a\beta\lambda}\right) \tag{15}$$

β is related to the Weissenberg number by:

$$\mathfrak{We} = \frac{3}{2a\beta\lambda}\left(1-\frac{\operatorname{atanh}(2a\beta\lambda)}{2a\beta\lambda}\right) \tag{16}$$

The characteristics of the liquid chosen for all simulations are 10^3 Pa.s for the viscosity and 10^3 kg/m^3 for density. For the Oldroyd-B model, the ratio λ_r/λ_t is 0.5. The inlet

flow is equal to 0.1 m/s. These conditions give 10^{-4} as Reynolds number and 300λ as Weissenberg number. With this geometry, we employ a mesh consisting of 40 960 elements.

The comparison between numerical and analytical profiles is given in Figure 3. The velocity profiles obtained are in good accordance and thus the code is validated.

In the case of the Phan-Thien and Tanner liquid, the velocity profiles are directly calculated from the equations (11) and (13). For the Giesekus liquid, the parameter β is determined by a non-linear square method from velocity equation (14). With these values of β, we calculate the new values of the Weissenberg number (16). In all cases, the gap between the values of the Weissenberg number is less than 0.6%. The velocity profile of Oldroyd-B liquid is similar to Newtonian fluid, i.e. parabolic profil.

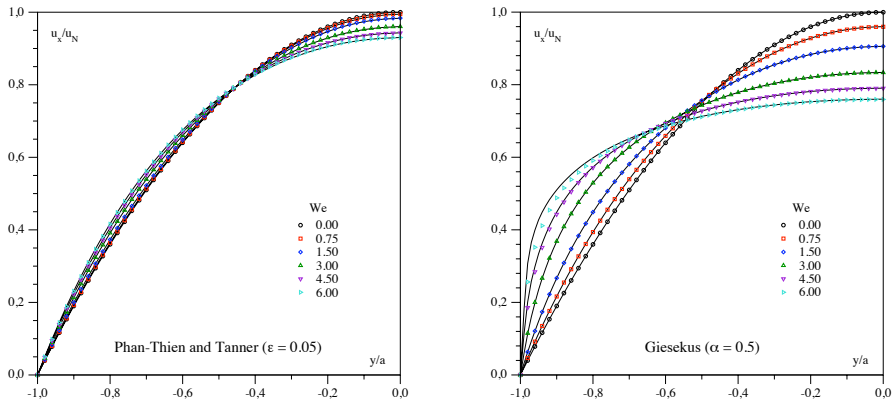

Figure 3: Profiles of the dimensionless velocity u_x/u_N vs. x/a with u_N the Newtonian velocity. 2D planar flow in a channel for a Phan-Thien and Tanner liquid, $\epsilon = 0.05$ and a Giesekus liquid, $\alpha = 0.5$. Comparison between numerical and analytical solutions.

4.4 4:1 abrupt contraction

A mesh of 32 768 elements corresponding to 17 089 nodes was used for these simulations. For our three fields formulation $(\boldsymbol{u}, p, \boldsymbol{\tau})$, the total number of unknows is 230 784.

Many polymeric liquid exhibit large recicurlating vortices upstream of the entry of an abrupt contraction. Our numerical simulations predict this phenomenon. The streamlines are presented in Figure 4. We observed a growth of vortices with increasing Weissenberg numbers. Lip vortex near the re-entrant corner is observed for Oldroyd-B liquid at $\mathfrak{We} = 6$.

In the case of Oldroyd-B and affine PTT liquids, 21 is the upper limit for the value of the Weissenberg number. For this value, the numerical results of velocities along the

plane of symmetry show oscillations after the contraction (Figure 5). This phenomenon is particularly significant in the case of Oldroyd-B model. On the other hand, any oscillations was observed for the Giesekus liquid and the value of 30 for the Weissenberg number was reached.

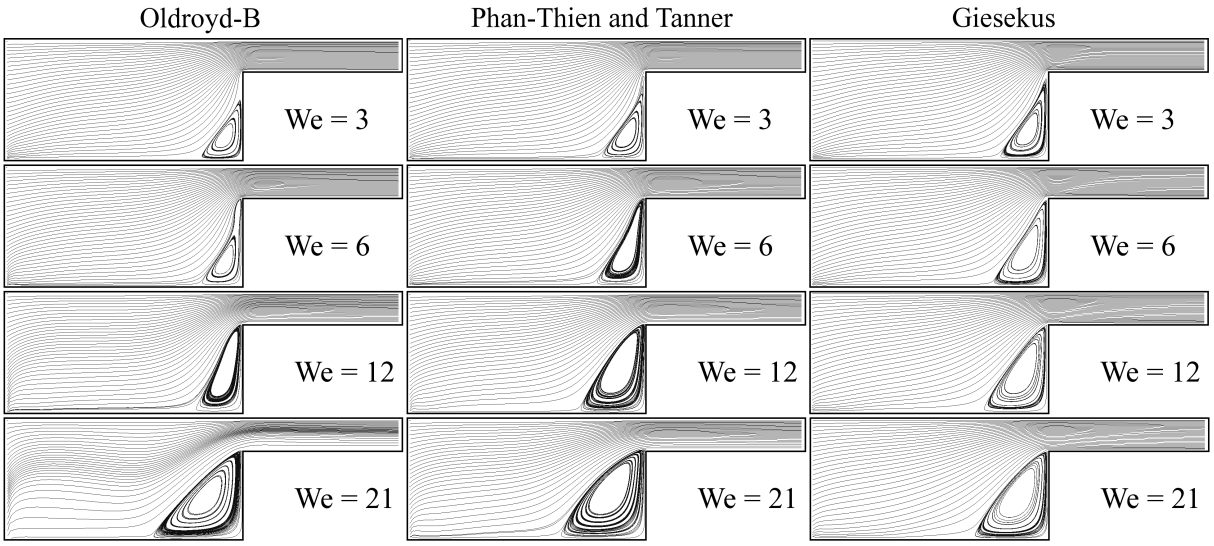

Figure 4: 4:1 contraction. Streamlines. Oldroyd-B ($\lambda_t/\lambda_r = 0.5$), Phan-Thien and Tanner ($\epsilon = 0.05$) and Giesekus ($\alpha = 0.5$) liquids.

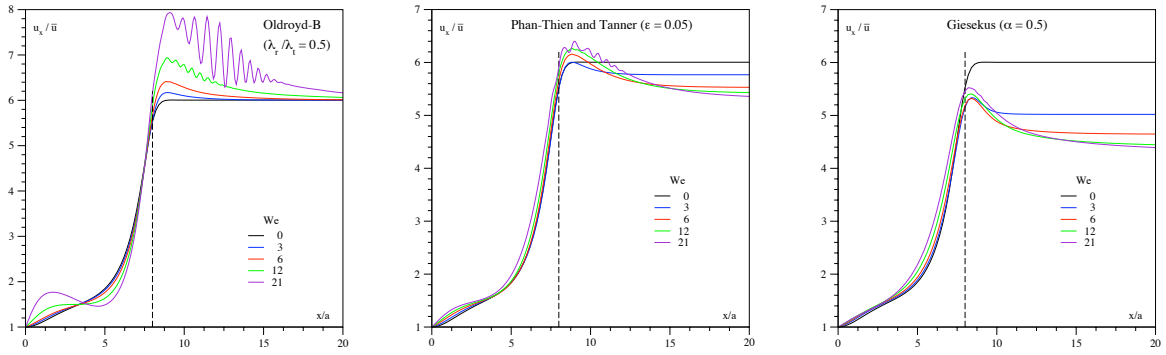

Figure 5: 4:1 contraction. $u_x/\overline{u}$ vs. x/a along the axis of symmetry. Oldroyd-B ($\lambda_t/\lambda_r = 0.5$), Phan-Thien and Tanner ($\epsilon = 0.05$) and Giesekus ($\alpha = 0.5$) liquids.

The elasticity of liquid is represented by the first normal-stress difference function. As this material function is a constant, $\Psi_1 = 2\eta\,(\lambda_t - \lambda_r)$ in Oldroyd-B case, the normal

stress increases dramatically with increasing Weissenberg number, i.e. $N_1 \propto \Psi_1 \dot{\gamma}^2$. The likely effect of normal stress on simulation is the loss of convergence. For the Giesekus model, the first normal-stress difference function is given by the following relationship:

$$\Psi_1(\dot{\gamma}) = \eta\lambda\sqrt{2}\,\frac{\sqrt{1+4\lambda^2\dot{\gamma}^2}-1}{\sqrt{1+\sqrt{1+4\lambda^2\dot{\gamma}^2}}}$$

In the high shear-rate range, the variation of this material function is proportional to $\dot{\gamma}^{1/2}$ and thus the normal stree is $\propto \dot{\gamma}^{3/2}$. In this case, the growth of the normal stress is smaller for the Giesekus liquid than the Oldroyd-B fluid.

The good stability of the numerical scheme used in the case of the Giesekus model might explain if we consider the conformation tensor[1]. The formulation used preserves the positivity of this tensor at the discrete level.

4.5 4:1:4 abrupt contraction/expansion

A mesh of 55 296 elements corresponding to 28 161 nodes was used for these simulations. For our three fields formulation $(\boldsymbol{u}, p, \boldsymbol{\tau})$, the total number of unknows is 388 096.

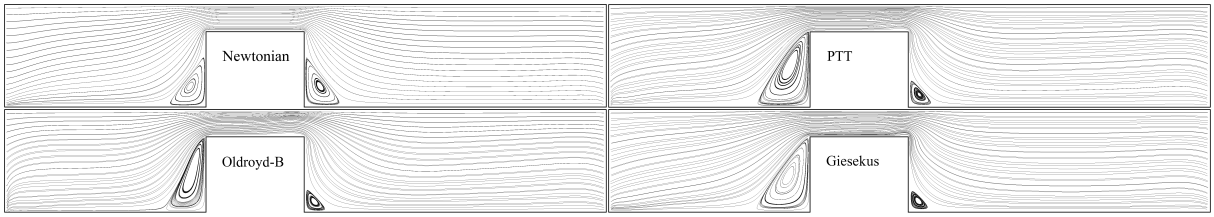

Figure 6: 4:1:4 contraction/expansion. Streamlines, $\mathfrak{We} = 12$. Oldroyd-B ($\lambda_t/\lambda_r = 0.5$), Phan-Thien and Tanner ($\epsilon = 0.05$) and Giesekus ($\alpha = 0.5$) liquids.

The streamlines are presented in Figure 6. Like the 4:1 contraction geometrie, we observed a growth of upstream vortices with increasing Weissenberg number and the formation of lip vortex near the re-entrant corner for Oldroyd-B liquid at $\mathfrak{We} = 6$.

Unlike the Newtonian liquid, there is a brutal decreasing of downstream vortices size in the viscoelastic cases. This result can fully be explained by the memory effect and the Weissenberg effect. the upper limit for the value of the Weissenberg number is respectively 16 for Oldroyd-B model, 21 for affine PTT model and > 30 for Giesekus model.

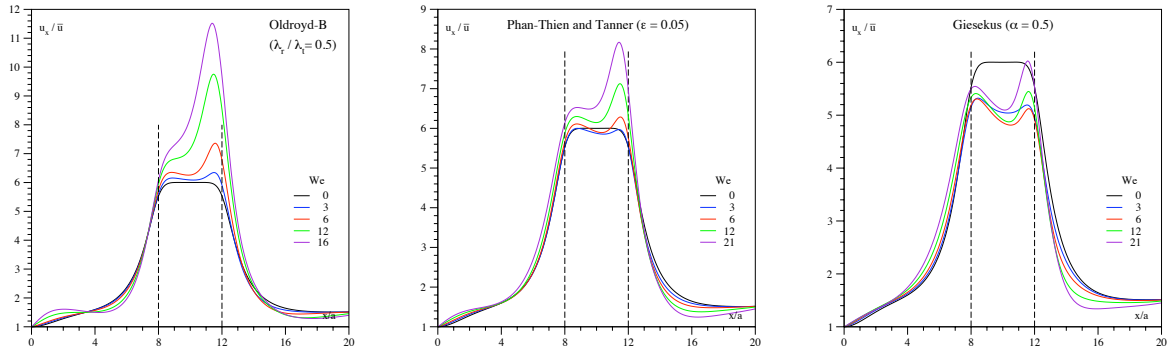

Figure 7: 4:1:4 contraction/expansion. $u_x/\overline{u}$ vs. x/a along the axis of symmetry. Oldroyd-B ($\lambda_t/\lambda_r = 0.5$), Phan-Thien and Tanner ($\epsilon = 0.05$) and Giesekus ($\alpha = 0.5$) liquids.

For this geometry, the numerical results of velocities along the plane of symmetry do not show oscillations (Figure 7).

REFERENCES

[1] Roland Becker and Daniela Capatina. Finite element discretization of the giesekus model for polymer flows. *Submitted in*, 2010.

[2] Roland Becker, Daniela Capatina, and Julie Joie. A dG method for the Stokes equations related to nonconforming approximations. Research report, INRIA Concha/UPPA, 2009.

[3] Oscar M. Coronado, Dhruv Arora, Marek Behr, and Matteo Pasquali. A simple method for simulating general viscoelastic fluid flows with an alternate log-conformation formulation. *Journal of Non-Newtonian Fluid Mechanics*, 147:189, 2007.

[4] M. Crouzeix and P.-A. Raviart. Conforming and nonconforming finite element methods for solving the stationary Stokes equations. I. *Rev. Française Automat. Informat. Recherche Opérationnelle Sér. Rouge*, 7(R-3):33–75, 1973.

[5] G. D'Avino, P. L. Maffettone, M. A Hulsen, and G. W. M. Peters. Numerical simulation of planar elongational flow of concentrated rigid particle suspensions in a viscoelastic fluid. *Journal of Non-Newtonian Fluid Mechanics*, 150:65, 2008.

[6] Raanan Fattal and Raz Kupferman. Constitutive laws for the matrix-logarithm of the conformation tensor. *Journal of Non-Newtonian Fluid Mechanics*, 123:281, 2004.

[7] H. Giesekus. A simple constitutive equation for polymer fluids based on the concept of deformation-dependent tensorial mobility. *Journal of Non-Newtonian Fluid Mechanics*, 11:69–109, 1982.

[8] H. Giesekus. Consitutive equations for polymer fluids based on the concept of configuration-dependent molecular mobility: a generalized mean-configuration model. *Journal of Non-Newtonian Fluid Mechanics*, 17:349–372, 1985.

[9] Martien A. Hulsen, Raanan Fattal, and Raz Kupferman. Flow of viscoelastic fluids past a cylinder at high Weissenberg number: Stabilized simulations using matrix logarithms. *Journal of Non-Newtonian Fluid Mechanics*, 127:27, 2005.

[10] M. W. Johnson Jr and D. Segalman. A model for viscoelastic fluid behavior which allows non-affine deformation. *Journal of Non-Newtonian Fluid Mechanics*, 2:255–270, 1977.

[11] Roland Keunings. On the high Weissenberg number problem. *Journal of Non-Newtonian Fluid Mechanics*, 20:209, 1986.

[12] Youngdon Kwon. Finite element analysis of planar 4:1 contraction flow with the tensor-logarithmic formulation of differential constitutive equations. *Korea-Australia Rheology Journal*, 16:183, 2004.

[13] R.G. Larson. *Constitutive equations for polymer melts and solutions*. Butterworths, Boston, 1988.

[14] Young-Ju Lee and Jinchao Xu. New formulations, positivity preserving discretizations and stability analysis for non-Newtonian flow models. *Computers methods in applied mechanics and engineering*, 195:1180, 2006.

[15] F. J. Lim and W. R. Schowalter. Pseudo-spectral analysis of the stability of pressure-driven flow of a Giesekus fluid between parallel planes. *Journal of Non-Newtonian Fluid Mechanics*, 26:135, 1987.

[16] Paulo J. Oliveira and Fernando T. Pinho. Analytical solution for fully developed channel and pipe flow of Phan-Thien-Tanner fluids. *Journal of Fluid Mechanics*, 387:271, 1999.

[17] N. Phan-Thien. A nonlinear network viscoelastic model. *Journal of Rheology*, 22(259), 1978.

[18] Nhan Phan-Thien and Roger I. Tanner. A new constitutive equation derived from network theory. *Journal of Non-Newtonian Fluid Mechanics*, 2:353–365, 1977.

[19] Jaap van der Zanden and Martien Hulsen. Mathematical and physical requirements for successful computations with viscoelastic fluid models. *Journal of Non-Newtonian Fluid Mechanics*, 29:93, 1988.

[20] K. Walters and M.F. Webster. The distinctive CFD challenges of computational rheology. *International Journal for Numerical Methods of Fluids*, 43:577, 2003.